Aging Effects on Heat Treatment Response and Mechanical Properties of Al-(1 to 13 pct)Si-Mg Cast Alloys

DIANA A. LADOS, DIRAN APELIAN, and LIBO WANG

The effects of artificial aging time on the mechanical properties of Al-Si-Mg cast alloys were investigated as a function of Si content and morphology. Five alloys with Si ranging from 1 to 13 pct, unmodified and Sr-modified, were tested systematically in as-cast, T4, and T61 conditions with different aging times. The results indicated that the ultimate tensile strength (UTS) and the yield strength (YS) increased with increasing aging time, and that the YS increased more than the UTS. The increase was low during the first 2 hours, significantly increased after 2 hours, and slowed down at ~10 hours; after 10 hours of aging, both UTS and YS remained nearly constant. The elongation decreased with increasing aging time. The decrease was observed from ~2 hours to ~14 hours, and no significant change was observed after ~14 hours. In T61 conditions with different aging times, UTS increased up to 24 pct, whereas YS increased up to 88 pct. The Si level had significant effects on UTS, YS, and elongation. For all aging conditions, alloys with a higher Si level had higher UTS and YS. Si content increased alloys' response to aging. Si modification also increased YS. The changes in mechanical properties were correlated to the fundamentals of the formation and evolution of Mg_2Si phase from forming clusters of Si atoms, GP zones, rod-like β' precipitates, and equilibrium Mg_2Si platelets.

DOI: 10.1007/s11663-010-9438-5

I. INTRODUCTION

THIS study is a part of an extensive investigation of the effects of heat treatment and Si content and morphology on the mechanical properties of Al-Si-Mg cast alloys. The effects of Si content/morphology and processing conditions during the solutionizing stage of the heat treatment were reported elsewhere.[1] It was shown that both Si content and morphology had a significant impact on mechanical properties as well as a strong influence on the alloys' response to solution treatment.[1] Here, the focus is on the effects of aging conditions and Si content and morphology on the microstructural changes and mechanical properties of this class of alloys. Although numerous articles have been written on the heat treatment of Al-Si-Mg alloys,[2–6] the literature lacks experimental data and a clear explanation of the effects of Si and other important processing parameters affecting the aging kinetics.

Cast Al-Si-Mg alloys may be used in a wide variety of tempers. For noncritical applications, castings may be put into service in the as-cast condition (F-temper) or with only a low-temperature T5 stabilization treatment. Most critical castings, however, generally are used in T6 or T7 heat-treated conditions. These treatments consist of solution treatment, quenching, and natural and artificial aging. Improvement in tensile properties is attributed mainly to the formation of the nonequilibrium Mg_2Si precipitates within the Al matrix.[7,8] In forming the strengthening Mg_2Si phase, solution treatment and quenching are the preparatory steps for aging. That is, during solution treatment, Mg and Si dissolve and homogenize in the Al matrix forming a solid solution, and as a result of the quench, Mg and Si form a supersaturated solid solution. The decomposition of the supersaturated solid solution occurs during aging, resulting in the formation of Mg_2Si precipitates, which enhance the yield and tensile strengths and affect various other properties. The precipitation sequence in Al-Si-Mg alloys can be represented as follows:

Needle-shaped Guinier–Preston (GP) zones (β'')
→ Rod-like β' precipitates (intermediary phases)
→ Equilibrium Mg_2Si platelets

The process begins with a clustering of Si atoms[9] leading to the formation of coherent spherical GP zones, which elongate along the cube matrix direction becoming needle-shaped.[10] The zones initially are disordered with a large vacancy concentration and become ordered with longer aging.[11] The needle-shaped GP zones correspond to monoclinic transition precipitates (β'').[12] GP zones are relatively stable and may exist up to a temperature of ~533 K (260 °C). With prolonged aging, the needle-shaped GP zones grow and form rods of an intermediary phase (β'). The β' particles are semicoherent with the matrix, and the rod axes are parallel to the cube matrix direction. The final equilibrium Mg_2Si phase (β) forms as incoherent platelets on the aluminum matrix and has an ordered face-centered

DIANA A. LADOS, Assistant Professor of ME and Director, is with the Integrative Materials Design Center, Worcester Polytechnic Institute, Worcester, MA 01609. Contact e-mail: lados@wpi.edu. DIRAN APELIAN, Howmet Professor of ME and Director, and LIBO WANG, Research Professor, are with the Metal Processing Institute, Worcester Polytechnic Institute.

Manuscript submitted August 26, 2010.
Article published online October 19, 2010.

cubic structure.[13] The peak hardness of the alloy is achieved before the platelets form.[14] The maximum size of the particles before the hardness begins to decrease is of the order of 0.03 μm.

The strengthening mechanism of Mg_2Si precipitates is accepted widely, but the literature does not have sufficient information showing the relationships between the amount of these precipitates and the mechanical properties of the material. Even though exact relationships cannot be determined, the effect of the Mg_2Si precipitates on properties can be estimated using relevant results from various studies. It has been reported in several studies that, in heat-treated Al-Si-Mg cast alloys, the increase in Mg up to a certain level improves mechanical properties, whereas additional increases do not affect or even slightly reduce the properties. For example, the study of Haque *et al.*[15] showed that maximum strength properties were obtained at ~0.4 pct Mg for both sand and permanent mold castings. Tsukuda *et al.*[16] showed that, in permanent molds, the ultimate tensile strength (UTS) and the yield strength (YS) of Na-modified alloys containing 0.2 pct and 0.006 pct Fe exponentially increased with Mg content up to 0.4 pct. In the same study, it also was reported that solution treatment and aging temperatures had a greater impact on the mechanical properties than Mg content. The study showed the importance of size and morphology of Mg_2Si and demonstrated that the effect of the amount of Mg_2Si precipitates cannot be fully understood without considering their size and morphology. This finding is likely the reason why no clear relations between the amount of Mg_2Si precipitates and the mechanical properties were provided. However, using the information in the literature, a trend and estimations can be given for this relation. The studies discussed[15,16] showed that the maximum UTS and YS are obtained at 0.4 pct Mg, which corresponds to the maximum of 0.63 pct Mg_2Si, assuming a sufficient amount of Si is present and that all supersaturated Mg is used. This implies that UTS and YS increase with the increase of Mg up to 0.4 pct or with the increase of amount of Mg_2Si precipitates to approximately 0.63 pct. When Mg is increased more than 0.4 pct or when Mg_2Si precipitates are increased more than 0.63 pct, the UTS and YS will not increase or may even decrease.

Previous studies have focused primarily on the effects of artificial aging temperature and time on properties. A systematic study on the aging behavior of an A356.2 alloy was carried out in the early 1990s in our laboratory.[3] Sand and permanent mold cast tensile bars were tested after being solution treated and aged at different temperatures for up to 100 hours. The hardness measurements showed that at an aging temperature of 298 K (25 °C) (natural aging) no hardening was observed for the first 0.5 hours after solution treatment. Subsequently, the hardness began to increase by 30 to 40 pct reaching the maximum value after approximately 2 days. The rate of hardening increased with temperature. At 444 K (171 °C) the hardness increased in the order of 60 to 70 pct in the first 2 to 3 hours, and subsequently, the changes observed occurred much slower. Generally, increasing time or temperature improved hardness, and increasing the temperature by 10 K (°C) was equivalent to increasing the aging time by a factor of two. Increasing aging time or temperature improved strength and lowered elongation. However, greater than 523 K (250 °C), sharp decrease in hardness occurred after 10 to 15 minutes. At 573 K (300 °C), the hardness decreased below the as-cast values in 0.5 to 1 hour.

At temperatures lower than ~448 K (175 °C), YS increased gradually with time, and a maximum value was attained after approximately 10 to 12 hours. At temperatures beyond this value, the hardening was rapid, and high YS could be observed even for a short aging time. Variation of the UTS with aging conditions was relatively small. The elongation decreased initially with aging time as the alloy hardened. However, at times longer than approximately 10 to 12 hours the elongation began to increase, and no significant reduction in strength was observed at this point. At temperatures higher than 453 K (180 °C) a substantial improvement in ductility was noted at prolonged aging, but strength decreased rapidly.

Studying Ti-grain refined A356 and A357 alloys, Misra *et al.* also found that elongation first decreased to a minimum, increased to a peak value, and then decreased again with longer aging periods.[4] This phenomenon occurred in specimens with secondary dendrite arm spacing (SDAS) of 30 to 50 μm for both alloys. The first minima values were shown at aging times of 7 to 11 hours, and the second peaks were reached at 12 to 14 hours. The secondary peaks were not found for specimens with large SDAS of 75 to 85 μm. Misra *et al.* found that, with prolonged aging time to reach the secondary elongation peak, the UTS and YS also increased. The electron microprobe and transmission electron microscopy analyses showed that during aging two types of precipitates were found in the aluminum—Mg_2Si and $TiAl_3$. The specimens contained only $TiAl_3$ and no Mg_2Si after solution treatment; Mg_2Si formed during aging. As the aging progressed, the relative distribution of Mg_2Si and $TiAl_3$ changed. The density of $TiAl_3$ continuously decreased, whereas that of Mg_2Si increased. At the lowest elongation point, equal distribution seemed to occur, and at the secondary elongation peak, only Mg_2Si was observed.

II. EFFECTS OF SI

The precipitation hardening of Mg_2Si took place much more rapidly in alloys containing excess Si.[17] The term "excess Si" refers to any Si dissolved in the solid solution exceeding the stoichiometric amount necessary for the formation of Mg_2Si precipitates. For example, 0.4 pct Mg in an alloy needs ~0.23pct Si to form Mg_2Si precipitates. Thus, in alloys with 0.4 pct Mg, when the Si content is greater than 0.23 pct, the alloy will contain excess Si (the solubility of Si in Al is approximately 1.4 pct at 811 K [538 °C]). Lynch *et al.*[18] pointed out that, during the first stage of precipitation, the composition of the precipitates in Al-Si-Mg system alloys could not be described as Mg_2Si but rather as $Mg_{0.44}Si$. To form $Mg_{0.44}Si$, 0.4 pct Mg requires ~1.05 pct Si.

This requirement implies that Si is one of the factors controlling the decomposition of the supersaturated solution, and the amount of Si dissolved in the α-solid solution influences Mg_2Si precipitation. When the concentration of Si in the supersaturated solution is high, the time required for the formation and growth of nuclei is short because of the reduced diffusion distances.

III. EXPERIMENTAL PROCEDURE

A. *Alloys*

The following alloys were produced and studied: Al-1Si-0.45Mg (alloy 1), Al-7Si-0.45Mg-unmodified (alloy 2), Al-7Si-0.45Mg-modified (alloy 3), Al-13Si-0.45Mg-unmodified (alloy 4), and Al-13Si-0.45Mg-modified (alloy 5). The compositions of the alloys are given in Table I. All casting conditions were designed appropriately to produce samples with constant SDAS of ~25 μm.

In the alloys studied, the Mg content was fixed at 0.45 pct. This Mg level is used commonly in A356 and 357 Al-Si-Mg cast alloys, which have combined Mg ranges from 0.17 to 0.7 pct. Also, based on the literature, 0.45 pct Mg content ensures that sufficient Mg_2Si precipitates can be produced for alloy strengthening during heat treatment. Three levels of Si (1, 7, and 13 pct) were selected for this study to create different amounts of Si eutectic structure. In Al-Si-0.45 pct Mg alloys, 1 pct Si does not form any eutectic Si structure, and it is sufficient for all 0.45 pct Mg to form Mg_2Si precipitates. The alloys with 13 pct Si produce the maximum amount of eutectic structure without forming primary Si particles. Whereas 7 pct Si alloys represent an intermediary condition akin to 356 alloys.

To create distinct Si morphologies for the unmodified and modified Si eutectic structures while maintaining the same grain size in all alloys (~300 μm), the amounts of Sr and Ti were controlled carefully using Al-10 pct Sr and Al-5 pct Ti-1 pct B master alloys (Table I). Because of its detrimental effects on mechanical properties, the Fe level was kept consistently below 0.02 pct (lower than the standard specification for 356 alloys). The remaining elements were kept at sufficiently low levels (<0.002 pct) to not introduce measurable effects on the mechanical properties of the alloys.

B. *Alloys and Test Specimens Preparation*

High-purity Al ingots and primary-grade master alloys were used. Measures were taken to keep the alloy compositions accurate and constant as well as mitigating melt contamination. The melts were rotary degassed with argon gas, and the hydrogen content after degassing was maintained at less than 0.1 cc/100 g for all alloys. Pouring temperatures were set at 983 K (710 °C) for alloys 4 and 5 (13 pct Si), 1018 K (745 °C) for alloys 2 and 3 (7 pct Si), and 1053 K (780 °C) for alloy 1 (1 pct Si). Different pouring temperatures were used to cast all alloys with the same superheat (~125 K [°C]) and fill the molds completely.

Standard tensile test specimens with 12.7-mm diameter (ASTM Standard B557) were cast in the vertically open-book die (Stahl mold) made of cast iron. The mold preheat temperature was approximately 723 K (450 °C) to 728 K (455 °C). For each alloy, 100 to 120 test bars were produced from four heats. In each heat, the alloy chemistry sample was taken halfway through the pour. The chemistries reported in Table I represent calculated averages, and the ± values represent the maximum variations among different heats and measurements.

C. *Heat Treatment*

The solution treatment was carried out at 811 K (538 °C) for 10 hours (typical solution treatment practice for A356 type alloys). The first part of this study[1] showed that for this condition all studied alloys gained maximum improvement in all mechanical properties and that the properties became less sensitive to solution treatment time. After solution treatment (including quenching), the specimens were left in air at room temperature (natural aging) for 12 hours and then (artificially) aged at 428 K (155 °C). For artificial aging, the ramp-up time to 423 K (150 °C) was ~1 hour, and 10 to 20 minutes more were needed to stabilize the temperature at 428 K (155 °C). Aging time was recorded once the temperature was stabilized; the temperature variation was ±1.5 K (°C). Eight aging times were tested from 2 to 16 hours with 2-hour intervals. At each preset time, the furnace was opened quickly, and the needed specimens were taken out and placed on the platform at ~298 K (25 °C). The door of the furnace was open for 3 to 4 seconds, after which the furnace temperature had a fluctuation of less than ±2 K (°C) for ~5 minutes. The solution-treated-only specimens (T4 condition) represent the 0-hour aging time condition.

D. *Tensile Testing and Microstructural Analysis*

Tensile tests were conducted according to the standard ASTM B 557 at room temperature. The strain was

Table I. Chemical Composition of Alloys

Alloy	Si	Mg	Ti	Sr	Fe	Others
Alloy 1	1.0 ± 0.1	0.45 ± 0.02	0.0070 ± 0.0005		<0.02	<0.002
Alloy 2	7.0 ± 0.1	0.45 ± 0.02	0.04 ± 0.005		<0.02	<0.002
Alloy 3	7.0 ± 0.1	0.45 ± 0.02	0.03 ± 0.005	0.019 ± 0.002	<0.02	<0.002
Alloy 4	13.0 ± 0.1	0.45 ± 0.02	0.28 ± 0.02		<0.02	<0.002
Alloy 5	13.0 ± 0.1	0.45 ± 0.02	0.22 ± 0.02	0.025 ± 0.002	<0.02	<0.002

measured using an axial extensometer with a gage length of 50.8 mm. The ramp rate was set at ~1 mm/min, and extensometer measurements were taken until the specimen was fractured. For each specimen, the UTS, YS, elongation (e pct), and modulus of elasticity (E) were derived and used in the study. For each alloy and each aging time, a minimum of five specimens were tested.

Vickers microhardness (HV) of the Al matrix was measured applying a load of 10 g for 10 seconds. An Optical microscope and scanning electron microscopy (SEM) were used for the phase morphology analysis, and energy-dispersive X-ray spectroscopy was used to identify different phases and their constituents.

IV. RESULTS

A. *Microstructure*

The microstructures for all alloys in as-cast and T61-treated (solution treated at 811 K [538 °C] for 10 hours, naturally aged for 12 hours, and artificially aged at 428 K [155 °C] for 12 hours) conditions are presented in Figure 1. The microstructures reveal significant differences between different alloys and between the as-cast and the heat-treated conditions of the same alloy. For the alloys with the same Si content, Si particles after T61 treatment are smaller and rounder in the modified conditions rather than in the unmodified conditions. Details on the microstructural variations of the alloys studied during solution treatment are given in the first part of the study.[1] The microstructure of the alloys changed significantly during solution treatment; however, during aging, no significant changes were observed via optical or SEM as the microstructural changes during aging consist primarily of the formation and evolution of Mg_2Si precipitates.

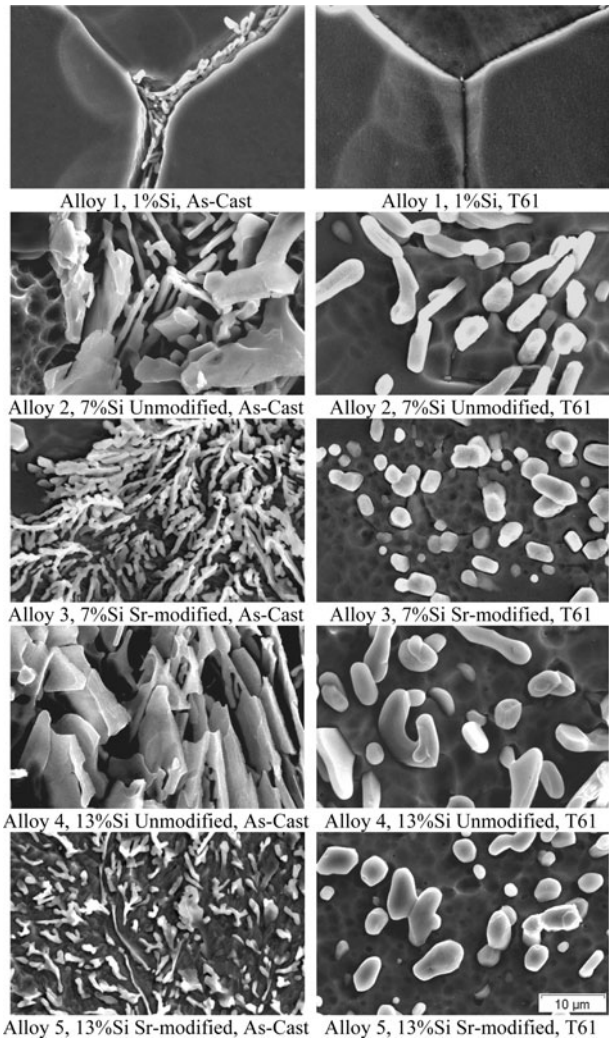

Fig. 1—Microstructures of the five studied alloys in as-cast (left) and T61 (right) conditions.

B. *Mechanical Properties*

1. *Microhardness of the Al Matrix*

Figure 2 presents the variations of the Al matrix microhardness with aging time for all alloys. The figure shows that the microhardness of the Al matrix increases with increasing aging time. In solution-treated conditions (T4, 0 aging time in Figure 2), the matrix hardness of the unmodified alloys (alloys 2 and 4) is similar. With aging, the hardness of all alloys increases, and generally, the alloy with the higher Si content has a higher hardness value. The difference becomes significant at approximately 2 hours of aging, remains nearly constant up to ~8 hours, and then narrows with prolonged aging. The increase in the matrix hardness of the 1 pct Si alloy is slow in the first few hours of aging, becomes faster at aging time from 8 to 12 hours, and then slows again after 12 hours. The matrix hardness of the modified alloys (alloys 3 and 5) is higher then that of the unmodified alloys (alloys 2 and 4) with the same Si content for the T4 and all aging conditions up to 16 hours. For modified alloys (alloys 3 and 5), the alloy with the higher Si content has a higher matrix hardness in T4 conditions. For both 7 and 13 pct Si-modified alloys, the hardness increases significantly and has a nearly constant difference at aging time from 2 to ~6 hours. Starting from approximately 6 hours for 13 pct Si-modified alloy and approximately 8 hours for 7 pct Si-modified alloy, their hardness increases become slower. After approximately 10 hours, their hardness becomes almost the same. Close to 16 hours of aging, the matrix hardness of all alloys becomes similar.

C. *Tensile Properties*

Figure 3 shows the variation of UTS, YS, and e pct with aging time for the 7 pct Si-modified alloy (alloy 3), which was solution treated at 811 K (538 °C) for 10 hours, naturally-aged for 12 hours, and artificially aged for different times. The data indicates that both UTS and YS increase with increasing aging time. For both the UTS and YS, the increasing rates are low in the first 2 hours, become higher in the 2 to 10 hours range, and then decrease to a slow rate after 10 hours. The difference is that the increase in YS is larger than the

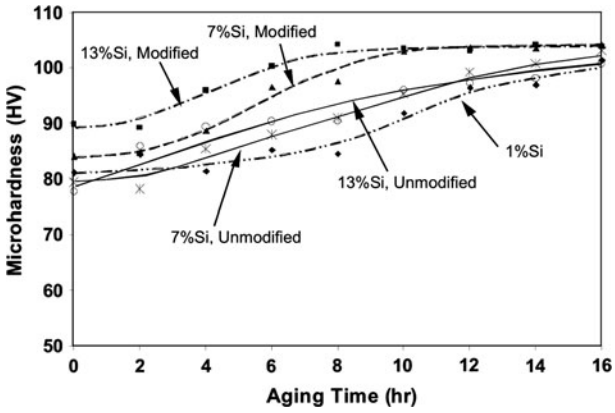

Fig. 2—Microhardness (HV) of the Al matrix *vs* aging time for all tested alloys.

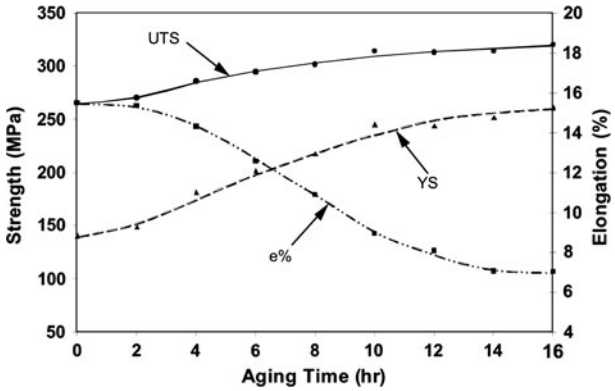

Fig. 3—UTS, YS, and e pct of the modified 7 pct Si alloy (alloy 3) *vs* aging time.

increase in UTS. For example, from the T4 condition to 16 hours of aging, the UTS increased ~21 pct (56 MPa), whereas the YS increased ~88 pct (122 MPa). The e pct values decrease with increasing aging time. The decrease starts at approximately 2 hours, accelerates between 2 and 12 hours, slows after 12 hours, and remains nearly unchanged after approximately 14 hours. From 0 (T4 condition) to 16 hours aging, the e pct decreased ~48pct (from 14.7 pct to 7 pct).

Figures 4, 5, and 6 show the variation of UTS, YS, and e pct with aging time for all alloys, which were solution treated at 811 K (538 °C) for 10 hours, naturally aged for 12 hours, and then artificially aged for different times. Table II lists the UTS, YS, and e pct of these alloys at aging times of 0, 2, 8, and 16 hours. Table III shows the increases in UTS and YS from 0 to 16 hours aging, and Table IV shows the variations of UTS and YS for different alloys at different aging times.

V. DISCUSSION

Aging effects are discussed with respect to the (1) variation in properties, UTS, YS, and e pct, with aging time; (2) effects of Si content; and (3) effects of the initial

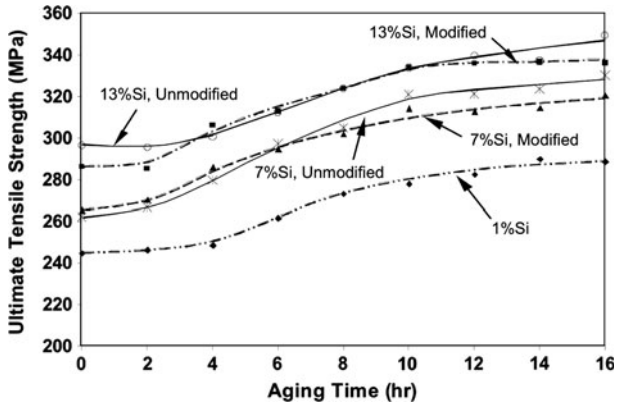

Fig. 4—Variation of UTS with aging time for all five studied alloys.

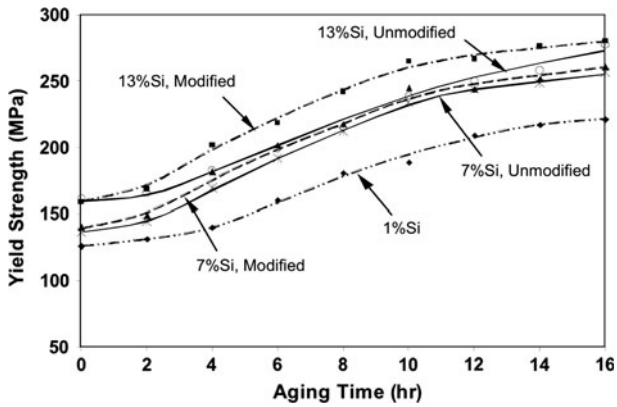

Fig. 5—Variation of YS with aging time for all five studied alloys.

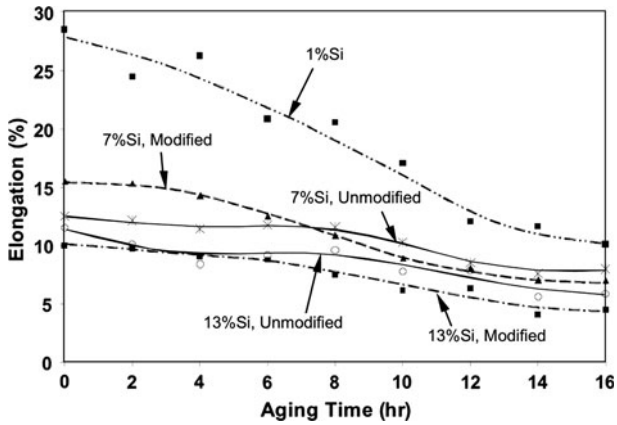

Fig. 6—Variation of e pct with aging time for all five tested alloys.

Si morphology on properties for different aging times, as follows:

(1) For all alloys, the variations in UTS, YS, and e pct with aging time are similar to those of the modified 7 pct Si alloy shown in Figure 3. Generally, in the first 2 hours, UTS and YS remain nearly constant and start to increase after 2 hours. The increase becomes slower around 10 hours, and thereafter,

Table II. Tensile Properties of the Alloys at Various Aging Times

	UTS – MPa (ksi)				YS – MPa (ksi)				e Pct			
	Aging Time (Hours)				Aging Time (Hours)				Aging Time (Hours)			
Alloy	0	2	8	16	0	2	8	16	0	2	8	16
Alloy 1 (1 pct Si)	244 (35.4)	246 (35.7)	273 (39.6)	289 (41.9)	128 (18.6)	132 (19.1)	181 (26.2)	221 (32.1)	27.1	24.4	20.6	10.1
Alloy 2 (7 pct Si unmodified)	264 (38.5)	267 (38.7)	305 (44.2)	330 (47.9)	139 (20.1)	145 (21.0)	212 (30.8)	256 (37.2)	12.0	12.1	11.6	8.0
Alloy 3 (7 pct Si Sr-modified)	264 (38.3)	270 (39.2)	302 (43.8)	321 (46.5)	139 (20.2)	150 (21.7)	218 (31.6)	261 (37.9)	14.7	15.4	10.9	7.0
Alloy 4 (13 pct Si unmodified)	300 (43.5)	295 (42.8)	324 (47.0)	350 (50.7)	165 (24.0)	165 (24.0)	215 (31.2)	278 (40.3)	12.1	10.1	9.6	5.9
Alloy 5 (13 pct Si Sr-modified)	284 (41.2)	285 (41.4)	324 (47.0)	336 (48.7)	157 (22.8)	169 (24.5)	242 (35.1)	281 (40.7)	10.7	9.8	7.5	4.5

Table III. The Increases in UTS and YS from 0 to 16 Hours of Aging

	UTS – MPa (ksi)				YS – MPa (ksi)			
	Aging Time (Hours)		Increase		Aging Time (Hours)		Increase	
Alloy	0	16	MPa (ksi)	Pct	0	16	MPa (ksi)	Pct
Alloy 1 (1 pct Si)	244 (35.4)	289 (41.9)	45 (6.5)	18.2	128 (18.6)	221 (32.1)	94 (13.6)	73.0
Alloy 2 (7 pct Si unmodified)	265 (38.5)	330 (47.9)	64 (9.3)	24.3	139 (20.1)	256 (37.2)	118 (17.1)	85.0
Alloy 3 (7 pct Si Sr-modified)	264 (38.3)	321 (46.5)	56 (8.1)	21.2	139 (20.2)	261 (37.9)	122 (17.7)	87.7
Alloy 4 (13 pct Si unmodified)	300 (43.5)	350 (50.7)	49 (7.1)	16.4	165 (24.0)	278 (40.3)	112 (16.3)	67.7
Alloy 5 (13 pct Si Sr-modified)	284 (41.2)	336 (48.7)	52 (7.5)	18.3	157 (22.8)	281 (40.7)	123 (17.8)	78.2

Table IV. Variations of UTS and YS for Different Alloys at Different Aging Times

	UTS – MPa (ksi)				YS – MPa (ksi)			
	Aging Time (Hours)			Increase From 0 to 8 Hours	Aging Time (Hours)			Increase From 0 to 8 Hours
Alloy	0	2	8	MPa (ksi)	0	2	8	MPa (ksi)
Alloy 1 (1 pct Si)	244 (35.4)	246 (35.7)	273 (39.6)	29 (4.2)	128 (18.6)	132 (19.1)	181 (26.2)	53 (7.6)
Alloy 3 (7 pct Si Sr-modified)	264 (38.3)	270 (39.2)	302 (43.8)	38 (5.5)	139 (20.2)	150 (21.7)	218 (31.6)	79 (11.4)
Alloy 5 (13 pct Si Sr-modified)	284 (41.2)	285 (41.4)	324 (47.0)	40 (5.8)	157 (22.8)	169 (24.5)	242 (35.1)	85 (12.3)

both UTS and YS remain nearly constant at prolonged aging times. Also, for the same alloy, the increase of YS is greater than the increase in UTS over the same time interval. For example, as shown in Table III, from 0 (T4) to 16 hours of aging, for all alloys, the UTS increases are in the range of 16 pct to 24 pct, whereas the YS increases are in the range of 68 pct to 88 pct.

(2) The effects of Si content on UTS and YS can be observed from two perspectives. First, at all aging times, the alloy with the higher Si content has a higher UTS and YS. Second, as mentioned previously, for all alloys, the UTS and YS increase with aging time from 2 to 10 hours, but the amounts of increase are different for alloys with different Si contents. Generally, the alloy with the higher Si content has a higher increase. Table IV shows comparisons between UTS and YS values of 1 pct Si as well as Sr-modified 7 and 13 pct Si alloys at aging time 0 (only solution treated and naturally aged), 2, and 8 hours. For these alloys, increases in YS from 0- to 8-hour aging are 53 MPa, 79 MPa, and 85 MPa, and in UTS, they are 29 MPa, 38 MPa, and 40 MPa, respectively. The data clearly point out that alloys with a higher Si content have larger increases in both UTS and YS with increasing aging time. Similar observations also hold true for UTS and YS of the unmodified alloys.

(3) In regard to the effects of initial Si particle morphology, Si modification does not have noticeable effects on UTS; the UTS of modified and unmodified alloys with the same Si content are similar in the aging range of 2 to 10 hours. However, Si modification has a significant effect on YS for

similar aging times. Even though the YS of modified and unmodified alloys with the same Si content are similar at 0 aging time (T4), the modified alloy has a higher YS beyond 2 hours of aging. The difference becomes larger with longer aging times until approximately 10 hours, after which the difference decreases and the behavior of the two alloys becomes similar.

For all alloys, the e pct does not show an obvious change in the first few hours of aging and then decreases with increasing aging time. For the 1 pct Si and the Sr-modified 7 and 13 pct Si alloys, the decrease starts after approximately 4 hours, and for the unmodified 7 and 13 pct Si alloys, the decrease starts at approximately 8 hours. For all alloys, the rates of decrease reduce after approximately 12 hours, and the e pct tends to remain constant at prolonged aging. The alloys with a lower Si content have a higher e pct for all aging times and generally have a greater decrease in e pct with aging time. Modification does not show a clear effect on e pct during aging.

The results suggest that, for Al-Si-Mg alloys aged at 428 K (155 °C), the incubation time of Mg_2Si precipitates formation is ~2 hours. During this time, the Si atoms supersaturated in the Al matrix start to cluster and form small amounts of coherent spherical GP zones. These incipient precipitates do not have a significant influence on the properties of the alloy. Aging times longer than 2 hours facilitate more GP zone formation, growth, and eventually transformation to rods of an intermediate phase (β'). The Si and Mg dissolved in the Al matrix is consumed to form GP zones, and because of the initial high concentrations of dissolved Si and Mg, the process starts fast, becomes slower, and finally stops as the supersaturated Si or Mg is consumed. The formation and evolution of the β' phase follows a similar pattern as the GP zones, except for the time delay; subsequently, β' phase gradually transforms to the equilibrium β phase. The alloys are strengthened mainly by the β' phase as well as by the GP zones, and the coarse equilibrium β phase does not have much strengthening effect. Thus, the variation in properties is mainly related to the amounts of β' phase and GP zones. It leads the matrix hardness, UTS, and YS of all alloys to start increasing at approximately 2 hours of aging; the increase is fast in the 2- to 8-hour range and then it slows around 10 hours. After 12 hours, the changes in properties are minor. The expected decrease in matrix hardness, UTS, and YS caused by the formation of the equilibrium β phase have not been observed in the 0- to 16-hour aging time regime investigated in this study.

The variation in e pct has an opposite behavior compared with UTS and YS. Elongation remains nearly constant in the first few hours of aging and then decreases. The decrease is fast at the beginning, but it becomes increasingly slower with increasing aging time. The results show that, to achieve the full strengthening effect in Al-Si-0.45 pct Mg alloys, the aging time should be 10 to 12 hours at 428 K (155 °C). Reduced aging time can result in higher e pct at the expense of reduced strength.

This work shows that alloys with a higher Si content not only have higher strength (UTS and YS) at all aging times, but that they also attain higher strength increases with increasing aging times. This finding suggests that Si increases the alloys' response to aging (*i.e.*, higher Si content resulting in a stronger response to aging). In addition, the initial Si size and morphology (as a result of the initial modification and solution treatment time and temperature) also influence the response to aging mainly for YS.

VI. CONCLUSIONS

The tensile properties of all tested alloys vary significantly with aging time. In the first 2 hours of aging at the selected solutionizing conditions, all properties remain nearly constant. This period is the incubation time for Mg-Si precipitates formation. Aging times longer than 2 hours facilitate GP zone (β'') formation, growth, and transformation to an intermediate phase (β'), which finally transforms to the coarse equilibrium Mg_2Si phase at prolonged aging time. The alloys are strengthened mainly by the GP zones and the β' phase; the equilibrium Mg_2Si phase does not have a significant strengthening effect. Thus, the UTS and YS start to increase after 2 hours. The increase becomes slower at ~10 hours, and thereafter, the values remain nearly constant at longer aging times. Generally, the e pct variation has the opposite trend compared with that of strength; when strengths increase, e pct decreases. For the same alloy, the increase in YS is greater than the increase in UTS over the same aging time interval.

Alloys with higher Si content have higher strengths (UTS and YS) at all aging times, and Si also increases the alloys' response to aging (*i.e.*, higher Si content results in a stronger response to aging). The initial Si size and morphology influences the alloy's response to aging, especially for YS.

ACKNOWLEDGMENTS

The authors gratefully acknowledge the member companies of the Advanced Casting Research Center (ACRC) for their support of this work and for their continued support of research focused on the science and technology of metal casting at Worcester Polytechnic Institute.

REFERENCES

1. D.A. Lados, D. Apelian, and L. Wang: *Metall. Mater. Trans. B*, 2010. DOI:10.1007/s11663-010-9437-6.
2. *ASM Handbook: Volume 4: Heat Treatment*, ASM, Materials Park, OH, 1991, pp. 849–50.
3. S. Shivkumar, C. Keller, and D. Apelian: *AFS Trans.*, 1990, vol. 98, pp. 905–11.
4. M.S. Misra and K.J. Oswalt: *AFS Trans.*, 1982, vol. 90, pp. 1–10.
5. D. Apelian, S. Shivkumar, and G. Sigworth: *AFS Trans.*, 1989, vol. 97, pp. 727–42.

6. H.J. Li, S. Shivkumar, X.J. Luo, and D. Apelian: *Cast Metals*, 1989, vol. 1 (4), pp. 227–34.
7. J.R. Davis: *Aluminum and Aluminum Alloys*, ASM, Materials Park, OH, 1993, pp. 297–98.
8. B. Closset, R.A.L. Drew, and J.E. Gruzleski: *AFS Trans*., 1986, vol. 94, pp. 9–16.
9. J. Lendvai, T. Ungar, and J. Kovacs: *Mater. Sci. Eng*., 1963, vol. 10, pp. 151–59.
10. H. Westengen and N. Ryum: *Metallfund*, 1979, vol. 70 (8), pp. 528–35.
11. R.J. Livak: *Metall. Mater. Trans. A*, 1982, vol. 13A, pp. 1318–21.
12. T. Shchegoleva: *Phys. Met. Metalloved*., 1968, vol. 25 (2), pp. 56–64.
13. E. Ozava and H. Kimura: *Acta Metall*., 1970, vol. 18, pp. 995–1006.
14. L.F. Mondolfo: *Aluminum Alloys: Structure and Properties*, Butterworth, London, UK, 1976.
15. M.M. Haque, G.H.J. Bennett, and V. Kondie: *Foundry Trade J*., 1983, pp. 387–90.
16. M. Tsukuda, M. Harada, T. Suruki, and K. Susumu: *JILM*, 1978, vol. 28 (3), pp. 109–15.
17. M. Kaczorowski: *Aluminum*, 1984, vol. 60, pp. E177–79.
18. J.P. Lynch, M. Brown, and H. Jacobs: *Acta Metall*., 1982, vol. 30, pp. 1389–94.